Scientific Research Publishing

Atmospheric and Climate Sciences, 2023, 13, 385-400
https://www.scirp.org/journal/acs
ISSN Online: 2160-0422
ISSN Print: 2160-0414

Calculations of Stratospheric Ozone and Effects of Diffusivity

Laurie Wei, Ibraheem Alelmi, Sen Nieh*

Department of Mechanical Engineering, The Catholic University of America, Washington, DC, USA
Email: *nieh@cua.edu

How to cite this paper: Wei, L., Alelmi, I. and Nieh, S. (2023) Calculations of Stratospheric Ozone and Effects of Diffusivity. *Atmospheric and Climate Sciences*, **13**, 385-400.
https://doi.org/10.4236/acs.2023.133021

Received: May 25, 2023
Accepted: July 15, 2023
Published: July 18, 2023

Abstract

This paper presents a system approach of mass balance of ozone and other species under diffusion-convection-reaction processes to study the ozone layer along the altitude in the stratosphere. The ozone abundance and general distribution above the tropical area were calculated and compared to the published measured data. The peak ozone layer was found to be 21 mPa at 22 km or 9.7 ppm at 30 km, and the involved competing processes depicting the ozone layer were explained in details. In the entire stratosphere from 10 km to 50 km, the calculated ozone distribution displayed a similar profile and trend to the observational data, with the calculation in ppm slightly above the measurement by 12%. The standard deviation of the differences between calculated and measured data was close to 0.25. A sensitivity study of gas diffusivities of molecular ozone D_3 and atomic oxygen D_1 on changing the ozone abundance and profile in the stratosphere showed that in the upper two-third of the stratosphere, D_1 evidently exhibited a pronounced impact on ozone, as much as 24-fold larger than D_3. The mechanism leading to this finding was also elaborated. The approach and calculations in this paper are shown to be useful for providing an initial insight into the structure and behavior of the complex ozone layer.

Keywords

Ozone, Stratospheric Distribution, Modeling, Diffusivity

1. Introduction

Being presented only in small trace amount, the stratospheric ozone is good and very important to human health and environmental sustainability, as it provides a protective layer to absorb the harmful high energy ultraviolet (UV) from the Sun. However, the small amount of ozone in the troposphere, particularly near

the ground, is known to be a polluting photochemical smog, which is bad to human, living beings, and the ecosystem [1].

The protective layer of stratospheric ozone was discovered by scientists to become thinner and depleted in many parts of the Earth [1] [2]. Ozone holes refer to areas with substantial ozone depletion in the stratosphere, originally found in the Antarctic, and later also found in the Arctic, and above the Tibetan mountains. The discovery and study of ozone distribution, behavior, depletion, and holes started in 1960s and has been ongoing today [1] [2] [3]. Ozone can be depleted and destroyed when it meets and reacts with nitrogen compounds and chlorine-containing chemicals, which is why traditional refrigerants used in HVAC and refrigeration, spray can propellants and blowing foam for cleaning, such as chlorofluorocarbons (CFCs) and hydrochlorofluorocarbons (HCFCs), are regarded as ozone depleting substances of reducing the protective stratospheric ozone.

CFCs can stay in the stratosphere for as long as 130 years. In the 1980s, scientists M.J. Molina and F.S. Rowland worked under P. Crutzen discovered the ozone hole and the link of chlorofluoromethane to the hole size based on their laboratory tests and computational modeling, which led to the Nobel Prize in Chemistry in 1995 [4]. The stratospheric ozone distribution across the globe varies with the geographical location, the altitude, and time and season of the year. The total ozone column above a location varies typically from 200 to 500 Dobson Units (DU), with a global average of 300 DU [5]. Ozone generation from solar UV radiation in the tropical areas is normally the strongest. However, the total ozone is reportedly a smaller value above the equator and larger values in the mid-latitudes and the polar region, because of the slow, large-scale horizontal circulation of ozone-rich stratospheric air taken from the tropical areas [1] [5].

To better understand the observational data of ozone and the underlying processes of ozone distribution and depletion caused by diffusion, convection, dynamic changes, and chemical reactions with species for ozone generation and consumption, various theoretical and numerical models were developed. One of the earliest models for ozone distribution and depletion was the Photochemical Box [6]. An example of a 2-D Photochemical Box model is the Global Ozone Chemistry and Related Trace Gas Data Activities model, which simulates the transport and chemistry of trace gases in the Earth's atmosphere, with a particular focus on the chemistry of ozone depletion [7]. The Photochemical Box model does not account for changes in wind patterns, temperature, and humidity, and its accuracy depends on the input parameters, such as the initial concentrations of atmospheric constituents and the intensity of the simulated sunlight. However, these parameters can be difficult to measure accurately, leading to uncertainties in the model predictions.

Several researchers of the Earth's atmospheric behavior and dynamics, including the ozone layer, employed 2-D models, focusing on in-depth study and

were used to solve a number of atmospheric chemistry and circulation-related issues [8]. The creation of increasingly complicated models with greater intricacy and depth, such as 3-D circulation patterns and chemical kinetics, has gained attentions in recent years [6]. These models may offer a more thorough knowledge of the ozone layer's behavior and provide more precise forecasts of future changes. However, while they provide a chemically based model for convection and diffusion, they do not show a focus on ozone behavior and distribution. Overall, 2-D models have proven a useful tool, but it's crucial to combine these models with observational data to fully comprehend the dynamics and behavior of the ozone layer [9].

Zonal mean models divide the atmosphere into latitude bands and calculate the average ozone concentration for each band [10]. It provides a simplified representation of the ozone layer and is useful for studying large-scale trends and patterns. An example is the Chemical Lagrangian Model of the Stratosphere, which uses a 2-D time-dependent framework to simulate the dynamics and chemistry of the stratosphere. One of its main advantages is their simplicity, with reduced computational power and is easier to set up and run. However, they do not account for regional variations in ozone concentration or the impact of atmospheric conditions to accurately represent the behavior of the ozone layer in certain regions or under certain conditions [8].

Latitude-altitude models, as compared to zonal mean models, provide a more detailed, accurate picture of the ozone layer along both latitude and altitude [11]. An example is the Canadian Middle Atmospheric Model, a 3-D chemistry-climate model that simulates the dynamics and chemistry of the middle atmosphere from the surface to the lower thermosphere. Ozone depletion modeling is used to project what the condition of the atmosphere will be in the future, given a reasonable starting point, by making use of equations for transport processes and rates of chemical reactions that are already known.

In this paper, we will use a general mass balance equation to account for the interactions of convection-diffusion-chemical reactions to focus on the study of ozone distribution and depletion. Although the modeling is an on-going, multi-dimensional approach for studying and better understanding the various underlying processes of ozone natural behavior and man-made depletion, the results discussed in this paper are of 1-D model and calculations, which have an inherent advantage of simplification and focusing only on ozone distribution, as compared to the measured data. In this case, major atmospheric properties and composition, and ozone-related physical-chemical processes are only a function of altitude, which makes it easier to interpret the complex results and study the specific processes of ozone behavior. This approach provides a higher resolution along the vertical structure of the atmosphere and the detailed processes along the latitude. It is computationally efficient and cost-effective, and believed to be useful in providing an initial insight into the complex dynamics of the ozone layer.

2. Modeling and Numerical Method

2.1. Mass Balance Equations

Ozone behavior and dynamics in the stratosphere are generally characterized by five competing processes in a mass balance equation, shown in Equations (1) to (3): photolysis, diffusion, convection, ozone generation reactions (Equations (4) to (5), listed in **Table 1(a)**) and ozone depletion reactions (Equations (6) to (10), listed in **Table 1(b)**) [3]. Photolysis is the process of solar radiation of energy $E = h\nu$, primarily UV, that breaks bonds of molecules of O_2, O_3, and other chemical species, where h being the Planck's constant, and ν being the frequency of the solar beam. This is the important initiating factor, as the intensity of UV depends on time of the day and season of the year, and the optical depth of the air mass penetrated, or the altitude. The stable, widely populated molecular oxygen O_2 (20.95% of air) is photo-chemically dissociated under high energy UV beam into two agitated atomic oxygen [O] as in Equation (4), and the dilute molecular ozone O_3 dissolved into O_2 and [O] as in Equation (7). Mass diffusion in space occurs when ozone, atomic oxygen or other species have a gradient in concentration in the stratosphere. Convection is involved in transport of ozone, atomic oxygen, and other species due to bulk flow of air in the stratosphere. Changes of ozone concentration or distribution can also be caused by various reactions involving the generation and destruction of ozone by natural processes and man-made chemical species [12] [13], as listed in **Table 1(a)** and **Table 1(b)**.

$$\begin{aligned}&\frac{\partial[\mathrm{O}]}{\partial t}+u\frac{\partial[\mathrm{O}]}{\partial x}-D_1\frac{\partial^2[O]}{\partial x^2}=\frac{\mathrm{d}[\mathrm{O}]}{\mathrm{d}t}\\&=k_1[\mathrm{O}][\mathrm{O}_2]-k_2[\mathrm{O}][\mathrm{O}_3]+k_3[\mathrm{O}_2]+k_4[\mathrm{O}_3]-k_7[\mathrm{ClO}][\mathrm{O}]\end{aligned} \tag{1}$$

$$\begin{aligned}&\frac{\partial[\mathrm{O}_2]}{\partial t}+u\frac{\partial[\mathrm{O}_2]}{\partial x}-D_2\frac{\partial^2[\mathrm{O}_2]}{\partial x^2}=\frac{\mathrm{d}[\mathrm{O}_2]}{\mathrm{d}t}\\&=k_1[\mathrm{O}][\mathrm{O}_2]+k_2[\mathrm{O}][\mathrm{O}_3]-k_3[\mathrm{O}_2]+k_4[\mathrm{O}_3]+k_5[\mathrm{O}_3][\mathrm{O}]\\&\quad+k_6[\mathrm{Cl}][\mathrm{O}_3]+k_7[\mathrm{ClO}][\mathrm{O}]\end{aligned} \tag{2}$$

$$\begin{aligned}&\frac{\partial[\mathrm{O}_3]}{\partial t}+u\frac{\partial[\mathrm{O}_3]}{\partial x}-D_3\frac{\partial^2[\mathrm{O}_3]}{\partial x^2}=\frac{\mathrm{d}[\mathrm{O}_3]}{\mathrm{d}t}\\&=k_1[\mathrm{O}][\mathrm{O}_2]-k_2[\mathrm{O}][\mathrm{O}_3]-k_4[\mathrm{O}_3]-k_5[\mathrm{O}_3][\mathrm{O}_3]-k_6[\mathrm{Cl}][\mathrm{O}_3]\end{aligned} \tag{3}$$

Since partial pressure and concentrations of molecular oxygen O_2 are very stable and large with an amount of 20.95% of air, of total pressure P_{Air} = 101,325 Pa at the sea level, or P_{Air} = 26,436 Pa at the bottom boundary of the stratosphere around 10 km, or P_{Air} = 76 Pa at the top boundary of stratosphere around 50 km, Equation (2) characterizing the changes of molecular oxygen, can be safely neglected and dropped, as compared to changes of partial pressure of ozone in the range of 0.02 Pa. The ozone-producing reactions in **Table 1(a)** lead to increases in ozone partial pressure in mPa (milli-Pascal = 10^{-3} Pa) and concentration in ppm (parts per million), while those ozone-consuming reactions in **Table 1(b)** lead to decreases in ozone partial pressure and concentration, by either natural processes or man-made ozone depleting chemical reactions.

Table 1. (a) Ozone-producing equations and nominal value of reaction rate constants, k_1 and k_3, of Equations (4)-(5) [1] [13]; (b) Ozone-consuming equations and nominal value of reaction rate constants, k_2 and k_4 - k_7, of Equations (6)-(10) [1] [13].

(a)

Reaction Equation	Equation No.	Reaction Rate Constant, k_i	Nominal Value, k_i
$O + O_2 \rightarrow O_3$	(4)	k_1	1.63×10^{-16}
$O_2 \rightarrow 2O$	(5)	k_3	Changes depending on time t

(b)

Reaction Equation	Equation No.	Reaction Rate Constant, k_i	Nominal Value, k_i
$O + O_3 \rightarrow 2O_2$	(6)	k_2	4.66×10^{-16}
$O_3 \rightarrow O + O_2$	(7)	k_4	Changes depending on time t
$2O_3 \rightarrow 3O_2$	(8)	k_5	8.60×10^{-16}
$Cl + O_3 \rightarrow ClO + O_2$	(9)	k_6	6.09×10^{-37}
$ClO + O \rightarrow Cl + O_2$	(10)	k_7	2.41×10^{-19}

As listed in Table 1, the reaction rate constants, k_1, k_2 and k_5 are constants that depend generally on the activation energies of O, O_2, and O_3, and temperature of the stratosphere, while k_3 and k_4 are constants that depend on UV beams at different time of the day and month of the year [1] [13]. Chlorine-related depleting chemicals from CFCs and HCFCs, simplified by Equations (9) and (10), with reaction rate constants k_6 and k_7, are included to quantify their effects of ozone depletion, as needed.

2.2. Numerical Solutions

Finite difference method for solving the mass balance equations in Equations (1) and (3), along with reaction equations in Equations (4) to (10), was employed in this paper. Assuming the Earth atmosphere is a closed system for ozone, the most concerned simultaneous processes of the two species, [O] (concentration of atomic oxygen) and [O_3] (concentration of ozone), are related to ozone changes in the stratosphere. The partial derivative terms of atomic oxygen and molecular ozone in Equations (1) and (3) can be expressed in finite differences, as $\frac{\partial O}{\partial x} = \frac{[O]_{i+1} - [O]_{i-1}}{2\Delta Z}$, $\frac{\partial O_3}{\partial x} = \frac{[O_3]_{i+1} - [O_3]_{i-1}}{2\Delta Z}$, $\frac{\partial^2 O}{\partial x^2} = \frac{[O]_{i+1} - 2[O]_i + [O]_{i-1}}{(\Delta Z)^2}$, and $\frac{\partial^2 O_3}{\partial x^2} = \frac{[O_3]_{i+1} - 2[O_3]_i + [O_3]_{i-1}}{(\Delta Z)^2}$, where ΔZ being the discretized change in altitude in the stratosphere, and Z ranging from 10 km to 50 km.

Assuming steady state condition ($\frac{\partial}{\partial t} = 0$), Equations (11) and (12) describe the simultaneous algebraic finite difference equations of the mass balance of O and O_3. The boundary conditions and parameters in the equations were given

based on practical selections as well as by Salawitch *et al.* [1]. Aside from altitude Z, such circumstances as, time of the day, temperature, air pressure, seasonal changes, wind speed u, diffusivity of atomic oxygen D_1 and diffusivity of ozone D_3, and initial atomic oxygen and ozone levels, were taken from the published data of measurements [1] [11]. For the photolysis process [13], the time of day is assumed the noontime of strong solar (and UV) radiation. From the measured data, for example, the concentrations at the lower boundary of stratosphere at $Z = 10$ km can be taken as [O] = 2 ppm and [O_3] = 7.93 ppm, and at the upper boundary of the stratosphere at $Z = 50$ km, [O] = 1.45 ppm and [O_3] = 2.5 ppm, respectively.

The concentrations of atomic oxygen [O] and ozone [O_3] in Equations (11) and (12) were calculated with a MATLAB code [3] along the altitude Z. The nonlinear term in Equations (11) and (12), $k_2[O][O_3]$, was solved by successive approximation iterations, where initial values of [O] and [O_3] were first guessed, and gradually modified according to the new values calculated in the previous run, till the difference between the two runs converged to an acceptably small value.

$$u\frac{[O]_{i+1}-[O]_{i-1}}{2\Delta Z}-D_1\frac{[O]_{i+1}-2[O]_i+[O]_{i-1}}{(\Delta Z)^2} = -k_1[O][O_2]-k_2[O][O_3]+k_3[O_2]+k_4[O_3]-k_7[ClO][O] \quad (11)$$

$$u\frac{[O_3]_{i+1}-[O_3]_{i-1}}{2\Delta Z}-D_3\frac{[O_3]_{i+1}-2[O_3]_i+[O_3]_{i-1}}{(\Delta Z)^2} = k_1[O][O_2]-k_2[O][O_3]-k_4[O_3]-k_5[O_3][O_3]-k_6[Cl][O_3] \quad (12)$$

3. Results and Discussions

3.1. Calculated vs. Measured Ozone O_3 without Depletion

Ozone O_3 was first discovered with a pungent smell in laboratory experiments in the mid-1800s [1]. It can react rapidly with many chemicals and is used for industrial bleaching and water purification. Being a gas naturally present in the atmosphere, stratospheric ozone was later confirmed by various chemical and optical measurement methods in the mid-1900s. **Figure 1** shows the calculated ozone partial pressure distribution along the altitude in the tropical area without man-made depletion processes [or $k_6 = 0 = k_7$ in Equations (9) and (10)], as compared to the measured ozone profile at the equator [5].

The solar UV radiation spectrum includes 1) very high energy UV-C (wavelength ranging from 100 to 280 nanometer, or nm), which is extremely harmful, but is entirely absorbed within the ozone layer, 2) high energy UV-B (280 to 315 nm), which is mostly absorbed by the ozone layer and can cause major damages to humans and living beings once it reaches the ground level, and 3) intermediate energy UV-A (315 to 400 nm), which is only slightly absorbed by the ozone layer. Exposure to UV-B increases the risks of skin cancer, cataracts, and deteriorated immune system, and extended exposure to UV-A may cause premature aging of the skin.

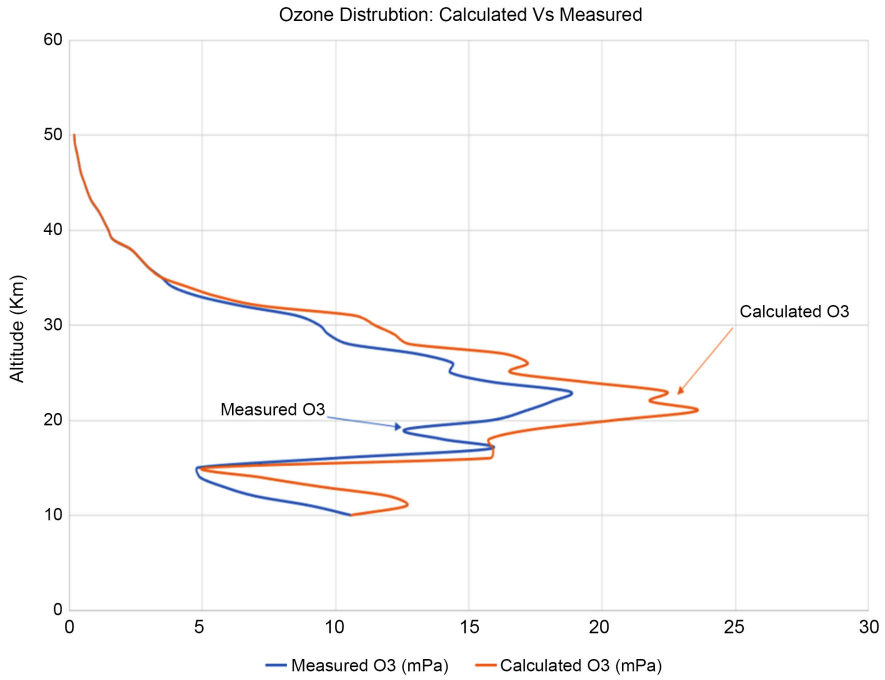

Figure 1. The calculated and measured ozone abundance in mPa along the altitude in the stratosphere (10 km - 50 km) in the tropical area show a similar profile and trend [5].

As shown in **Figure 1**, ozone abundance in mPa starts at low values in the upper part of the stratosphere (35 km - 50 km), and increases to 21 mPa around Z = 22 km, which indicates the richest layer or the peak of the stratospheric ozone. It decreases to the lowest value of 4 mPa around 14 km, and reverts back slightly to 10 mPa at the bottom boundary of the stratosphere around 10 km. In the upper part of the stratosphere, the incoming solar beam, primarily UV-C and some UV-B, initiates the photolysis of molecular oxygen O_2 to turn into two atomic oxygens O, as in Equation (5). The chemically active atomic oxygen O collides with abundant O_2 to form molecular ozone O_3, as in Equation (4). As more atomic oxygen is generated by high energy UVs, more ozone will be formed, until the maximal abundance of ozone is reached around 22 km (the lower one-third of the stratosphere). As UV radiation beams into the stratosphere, it is absorbed with its intensity weakened with the depth of air mass penetrated. Meanwhile, as more O_3 is generated with an increased concentration, the ozone-depletion reactions in Equations (6), (7) and (8) become increasingly prominent which consumes and reduces the formed ozone. With the presence of man-made ozone-depleting species in Equations (9) and (10), more ozone will be depleted in an increased rate in the lower part of the stratosphere. In addition to ozone related chemical reactions, physical processes of mass diffusion from concentration gradient and convective transport of mild air flow, can also change the distributions of ozone in the stratosphere. **Figure 1** also shows the calculated ozone distribution in mPa, along with the measured ozone values [1] along the altitude. In the entire stratosphere from 10 km to 50 km, the calculated

distribution displays a similar profile and trend as compared to the measured results. The measured data of ozone were from Newman *et al.* [5], collected from NASA Goddard Space Flight Center using MERRA-2, to simulate the GEOS Atmospheric Model.

Both calculated and measured ozone partial pressures (in mPa) and ozone concentrations (in ppm) along altitude Z in the stratosphere are listed in Table 2, where the average values and standard deviations of calculations and measurements can be quantified. In addition to a similar trend of the profiles shown in Figure 1, the calculated results were found to have an average ozone partial pressure of 8.89 mPa, slightly higher than the measured average of 7.22 mPa. As listed in Table 2, the standard deviation of 0.25 is the root mean square of the dimensionless differences between the calculated and measured values, which shows how close of the calculated profile and the measured profile.

To convert partial pressures of ozone P_{Ozone} in mPa to concentrations of ozone in air [O_3] in ppm, Figure 2 shows the measured air temperature T, total pressure P_{Air}, and air material density ρ_{Air} along altitude Z in stratosphere and troposphere [12].

Both air density ρ and total air pressure P decrease rapidly as it ascends in the atmosphere. For example: ρ_{Air} = 1.225 kg/m^3, P_{Air}= 101,325 Pa = 1.01 × 10^8 mPa, and T = 15˚C at the ground level; ρ_{Air} = 0.4127 kg/m^3, P_{Air}= 2.64 × 10^7 mPa, and T = −50˚C at the bottom boundary of the stratosphere at 10 km; ρ_{Air} = 0.07 kg/m^3, P_{Air}= 4.3 × 10^3 mPa, and T = −54.5˚C at the peak of the ozone layer in stratosphere around 22 km; and ρ_{Air} = 0.001 kg/m^3, P_{Air}= 76 mPa, and T = −2.5˚C at the top boundary of stratosphere at 50 km. In the troposphere, the air temperature drops steadily from the ground value of around 15˚C at an elapsed rate of −6.5˚C/km to around −56.5˚C at tropopause between 10 km to 15 km. Because the solar energy is trapped and absorbed by greenhouse gases in the stratosphere, air temperature reverts and warms up to −15˚C at the two-third from the bottom of the stratosphere before it cools down to −2.5˚C at the top of stratosphere, as shown in Figure 2.

Table 2. The calculated and measured [5] ozone abundance in ppm and mPa along the altitude Z in the stratosphere above the equator.

Altitude	*Ozone, ppm*			*Ozone, mPa*		
Z, km	Measured	Calculated	$[(C - M)/M]^2$	Measured	Calculated	$[(C - M)/M]^2$
50	2.50	2.50	0.00	0.19	0.19	0.00
49	2.75	2.75	0.00	0.22	0.22	0.00
48	3.00	3.00	0.00	0.30	0.30	0.00
47	3.30	3.30	0.00	0.37	0.37	0.00
46	3.70	3.70	0.00	0.44	0.44	0.00
45	4.00	4.00	0.00	0.57	0.57	0.00
44	4.30	4.30	0.00	0.69	0.69	0.00

Continued

43	4.70	4.70	0.00	0.85	0.85	0.00
42	5.00	5.00	0.00	1.10	1.10	0.00
41	5.15	5.15	0.00	1.29	1.29	0.00
40	5.30	5.30	0.00	1.47	1.47	0.00
39	5.50	5.50	0.00	1.65	1.65	0.00
38	5.75	5.75	0.00	2.30	2.30	0.00
37	5.90	5.90	0.00	2.66	2.66	0.00
36	6.00	6.00	0.00	3.00	3.00	0.00
35	6.20	6.20	0.00	3.47	3.47	0.00
34	6.50	7.43	0.02	3.90	4.46	0.02
33	7.00	7.95	0.02	4.90	5.57	0.02
32	7.50	8.37	0.01	6.51	7.27	0.01
31	7.75	9.74	0.07	8.53	10.71	0.07
30	8.00	9.77	0.05	9.38	11.45	0.05
29	7.50	9.39	0.06	9.75	12.21	0.06
28	7.00	8.51	0.05	10.50	12.77	0.05
27	6.50	8.14	0.06	13.00	16.28	0.06
26	6.00	7.17	0.04	14.40	17.21	0.04
25	5.70	6.60	0.02	14.31	16.57	0.02
24	5.30	6.46	0.05	15.90	19.38	0.05
23	4.70	5.60	0.04	18.80	22.40	0.04
22	4.20	5.04	0.04	18.15	21.78	0.04
21	3.50	4.81	0.14	17.15	23.57	0.14
20	2.90	3.74	0.08	15.88	20.48	0.08
19	2.10	2.89	0.14	12.60	17.34	0.14
18	2.00	2.25	0.02	14.00	15.75	0.02
17	1.80	1.81	0.00	15.82	15.90	0.00
16	1.00	1.58	0.34	10.00	15.80	0.34
15	0.40	0.43	0.01	4.82	5.18	0.01
14	0.35	0.51	0.21	4.90	7.14	0.21
13	0.35	0.57	0.40	5.78	9.41	0.40
12	0.35	0.60	0.51	7.00	12.00	0.51
11	0.40	0.56	0.16	9.05	12.67	0.16
10	0.40	0.40	0.00	10.57	10.57	0.00
Average	**4.20**	**4.72**	**0.06**	**7.22**	**8.89**	**0.06**
			Standard Deviation = 0.25			**Standard Deviation = 0.25**

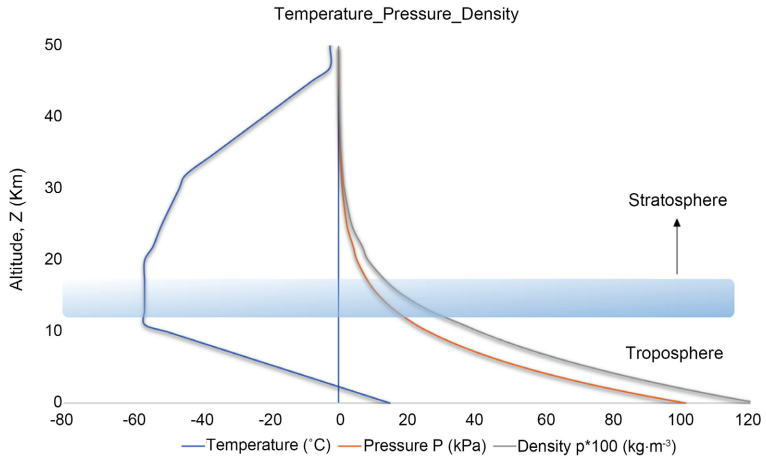

Figure 2. Measured air temperature T, total pressure P, and air density ρ along altitude Z in the troposphere and the stratosphere [12].

From the data in **Table 2**, **Figure 3** plots the calculated ozone distribution in ppm as compared to the measured ozone values along the altitude Z. Ozone concentration in ppm can be calculated to give the partial pressure of ozone P_{Ozone} divided by air pressure at the same altitude, or $[O_3] = P_{\text{Ozone}}(Z)/P_{\text{Air}}(Z) \times 10^6$. Similar to **Figure 1**, **Figure 3** shows in the stratosphere, the calculated ozone concentration exhibiting a similar profile and trend, as compared to the measured data. However, the peak of the profile occurs around $Z = 30$ km, where the calculated value of 9.77 ppm over the measured value of 8.0 ppm. The peak and the ozone profile shift to a higher altitude, from 22 km to 30 km, because of the decreasing air pressure as the altitude ascends. The calculated results of ozone concentration were found to have an average value of 4.72 ppm in the stratosphere, slightly by 12% above the measured average of 4.2 ppm. As seen in **Table 2**, the standard deviation is 0.25, which shows the calculated results are close within 25% of the measured data.

3.2. Calculated vs. Measured Atomic Oxygen [O] in the Stratosphere

Figure 4 shows the calculated atomic oxygen concentrations [O] along the altitude Z in ppm, as compared to the measured data [5]. The agitated atomic oxygen [O] is generated from the photolysis of high energy UV-C or UV-B of solar radiation in Equations (5) and (7). Beer's law of radiation [14] states that as the UV beam goes through the stratosphere, it is partially absorbed and its intensity attenuates with the optical depth of the air mass. As the generation of [O] slows down with the weakened UV, it is consumed to either generate ozone and atomic chlorine, or to deplete ozone, as in Equations (4), (6), and (10).

Figure 4 describes the effect of UV rays on atomic oxygen [O] which would sensitively affect ozone levels. Similar to $[O_3]$, **Figure 4** shows the calculated atomic oxygen concentration [O] follows the profile and trend of the measured [O]. It increases and reaches the peak of 9.7 ppm in the mid-altitude of the stratosphere around $Z = 30$ km, and then is rapidly consumed and decreases to 0.5

ppm near the bottom of the stratosphere.

3.3. Effects of Gas Diffusivity on Stratospheric Ozone

While stratospheric ozone abundance and its vertical distribution can be affected by many factors: chemical composition and temperature of the stratosphere, change of UV beam, amount of atomic oxygen and ozone-depleting species, etc., this paper presents a sensitivity study of gas diffusivities on ozone distribution, specifically diffusivity of ozone D_3 and diffusivity of atomic oxygen D_1. Ozone concentrations in ppm were calculated along the altitude of the stratosphere with different values of gas diffusivity, deviating from the nominal values of D_1 = 0.05 km^2/s and D_3 = 0.005 km^2/s [5].

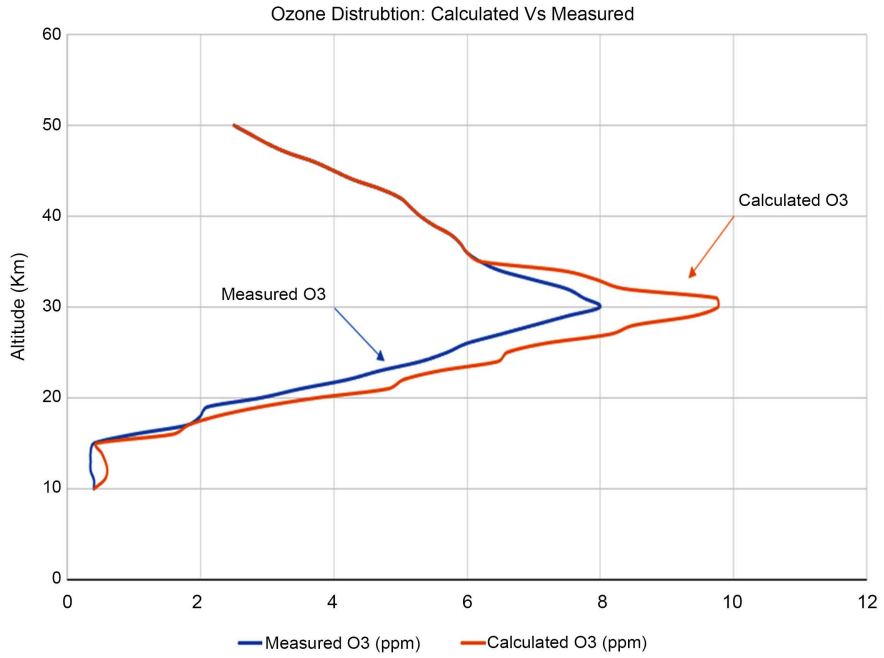

Figure 3. The calculated and measured ozone abundance in ppm along the altitude Z in the stratosphere in the tropical area show a similar profile and trend [5].

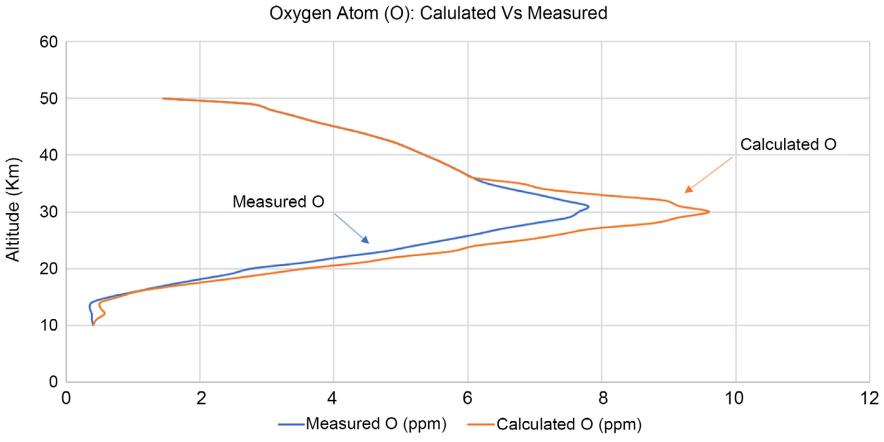

Figure 4. The calculated and measured atomic oxygen in ppm along the altitude Z in the stratosphere in the tropical area show a similar profile and trend [1] [3].

When parameters and boundary conditions of the equations ($[O_3]$ = 10 ppm, [O] = 0.4 ppm at Z = 10 km and $[O_3]$ = [O] = 0 ppm at Z = 50 km), including ozone diffusivity D_3 = 0.005 km^2/s, are kept constant, Figure 5(a) shows a family of curves of ozone distribution for different values of atomic oxygen diffusivity (D_1). The stratospheric ozone profile at small D_1 is not as high at higher altitudes as those of large D_1. As seen in Figure 5(a), with a change of 0.005 km^2/s of D_1, from −20%, to −10%, to 0%, to 10%, and to 20% of D_1, it is clear, particularly at higher altitudes, ozone concentrations fan out and increase significantly. For D_1 = 0.04 km^2/s (80% of nominal D_1), ozone concentrations remain below 18 ppm at all altitudes, with a peak at Z = 35 km, while for D_1 = 0.06 km^2/s (120% of nominal D_1), ozone concentrations are much larger and reach the peak of 28 ppm at an altitude shifting to higher stratosphere at Z = 40 km. The effect of D_1 on ozone distribution is evidently sensitive, which is believed to be caused by stronger dispersion of [O] in the upper half of the stratosphere that increases the ozone generation.

To quantify the effect of varied diffusivity of ozone D_3 on stratospheric ozone distribution, parameters and boundary conditions, including atomic oxygen diffusivity D_1 = 0.05 km^2/s were kept constant, while the diffusivity of ozone D_3 was varied by 0.0005 km^2/s of D_3, from −20%, to −10%, to 0%, to 10%, and to 20% of D_3, as shown in Figure 5(b). Opposite to the change of D_1, as D_3 level increased, the ozone concentration levels decreased in a small scale. Moreover, the ozone concentration for small D_3 (0.004 km^2/s) is only slightly larger than that of large D_3 (0.006 km^2/s). All five curves of changes of 80% to 120% of nominal D_3 = 0.005 km^2/s remain very close, with the peak ozone concentrations of around 19 ppm at a higher-altitude of Z = 38 km. This influence is consistent and as expected that a larger D_3 enhances the zone of higher ozone concentration to diffuse to zones of lower concentration both above and below the peak altitude, that leads to a more uniform distribution of stratospheric ozone. However, the small value of diffusivity D_3 = 0.005 km^2/s of a heavier triatomic ozone (molecular weight being 48 g/cm^3-mole) in a lighter air (molecular weight being 28.9 g/cm^3-mole), the level of physical diffusion in space will be low.

Figure 5(c) further compares the ozone concentrations under different levels of gas diffusivity from D_1 = 0.04 km^2/s, D_3 = 0.004 km^2/s to D_1 = 0.06 km^2/s, D_3 = 0.006 km^2/s. In the lower one-third of the stratosphere, Z < 25 km, diffusivities of both D_1 and D_3 were found to exhibit a negligibly small impact on ozone concentrations and profiles. However, as Z levels increased above 25 km, particularly Z > 30 km, in the upper part of the stratosphere, atomic oxygen diffusivity D_1 exhibited a pronounced impact on ozone distribution than D_3, until the altitude reached above 47.5 km, before the different diminishing to 0 at Z = 50 km.

As seen in Figure 5(c), ozone concentration changes by 20% deviation of D_1 were less than the changes of 20% deviation of D_3 in the lower stratosphere, 10 km < Z < 20 km. The changes of ozone at Z = 25 km were +0.8 ppm by D_1 and −0.7% by D_3, about the same rate. When ascending above Z = 25 km, the deviation

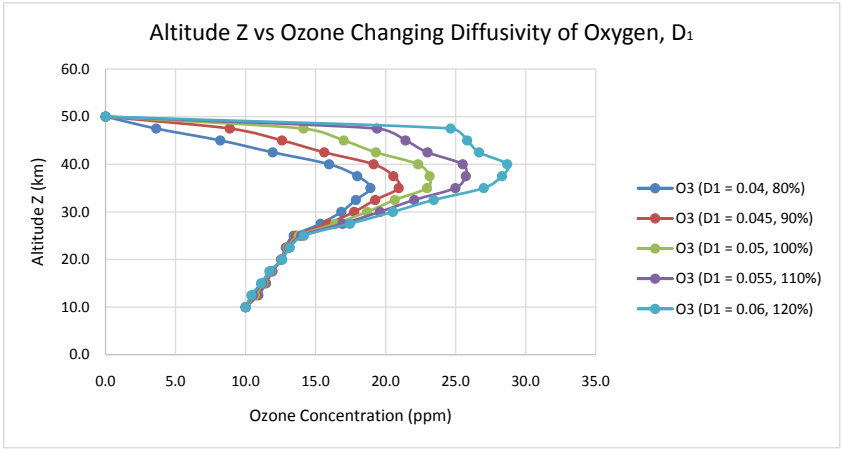

(a)

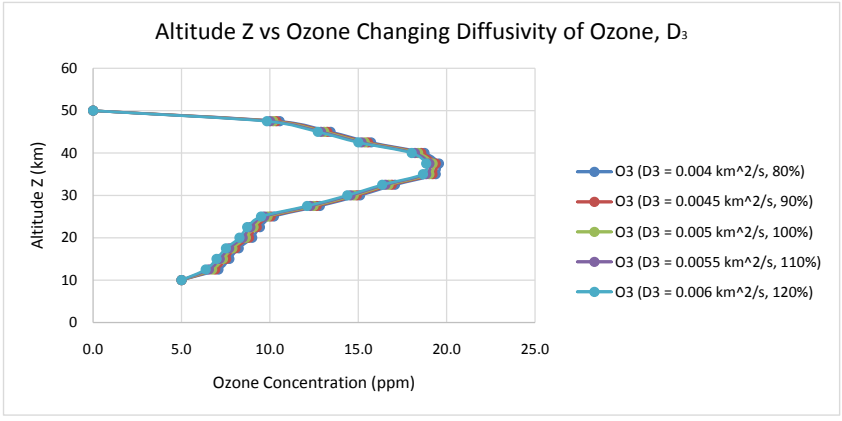

(b)

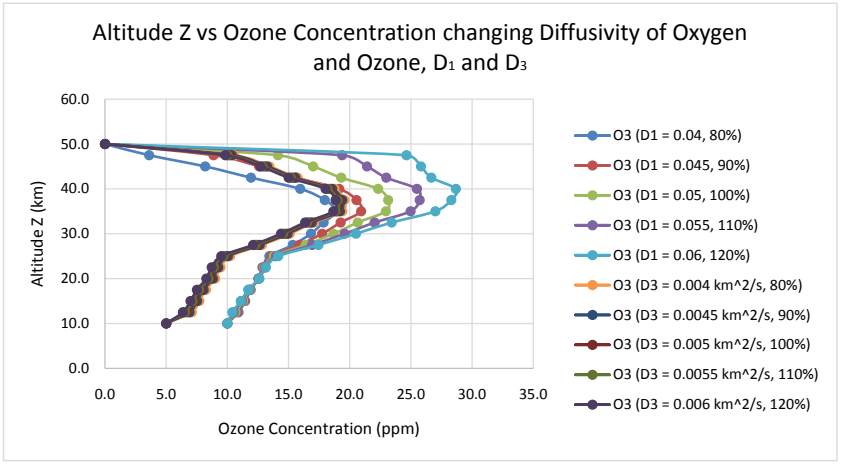

(c)

Figure 5. (a) The effect of diffusivity of atomic oxygen D_1 on the calculated ozone distributions, with diffusivity levels at D_1 = 0.04 (80%), 0.045, 0.05 (100%), 0.055, and 0.06 (120%) km^2/s; (b) The effect of ozone diffusivity D_3 on the calculated ozone distribution, with different diffusivity levels at D_3 = 0.004 (80%), 0.0045, 0.005 (100%), 0.0055, and 0.006 (120%) km^2/s. (c) Sensitivity study of the effects of diffusivities of atomic oxygen D_1 and ozone D_3 on ozone distributions in the stratosphere, with values of D_1 ranging from 0.04 to 0.06 km^2/s, and D_3 from 0.004 to 0.006 km^2/s.

of D_1 were found to exhibit much stronger impact on ozone abundance and its distribution than the deviation of D_3. The changes of ozone at $Z = 35$ km were +8.1 ppm by D_1 and −0.7 ppm by D_3, about 11-fold difference. At $Z = 45$ km, influence of D_1 on ozone was most apparently and amounted to 12.7 ppm over that by D_3 of −0.7 ppm. The profound impact of D_1 on ozone distribution amounted clearly to 24-fold larger than that of D_3. The sensitivity of gas diffusivity of atomic oxygen D_1 over that of ozone D_3 on controlling the ozone vertical profile in the stratosphere is evident.

The findings on the effect of gas diffusion on ozone above are believed to be related to the competing physical-chemical processes in the stratosphere. In the upper part of the stratosphere, ozone O_3 production by atomic oxygen O, in Equation (5), is the main process, which is closely associated with the photolysis of oxygen O_2 by UV radiation. A large diffusivity of agitated atomic oxygen D_1 encourages the dispersion of [O] in the upper stratosphere that collides more effectively with oxygen to generate more ozone, as in Equation (4). The ozone–depleting reactions in **Table 1(b)** are not important because of low concentration of ozone in the upper stratosphere. However, in the lower part of the stratosphere, the intensity of UVs is weakened, and with more ozone has produced, ozone-depleting reactions, in Equations (6), (8), and (9), add in and become strong to consume the formed ozone to counter the increase of ozone concentration. Ozone abundance increases when the parallel competing processes favor ozone production over the consumption, and vice versa. The stratosphere-troposphere exchangesand turbulent diffusion of ozone and chemical species [15] may also play a part of the influence of diffusivity in **Figure 5(c)**.

4. Summary

To better understand the observational data and the underlying processes of stratospheric ozone causedby photolysis, mass diffusion, convective transport, and ozone-generating and depleting chemical reactions, a system approach of mass balance of ozone and other species was employed to focus on the study of ozone distribution, behavior, and depletion. Although the modeling effort is an on-going, multi-dimensional approach, the results presented in this paper are of one-dimensionalmodel and calculations of detailed ozone and atomic oxygen distributions along the latitude of the stratosphere. This simple, computationally efficient approach helps provide an initial insight into the complex dynamics of the ozone layer.

As shown in **Figure 1** and **Figure 3**, the calculated results, validated by the measured data, depict that both ozone abundance expressed as ozone partial pressure in mPa or ozone concentration in ppm start slowly at low values in the upper part of the stratosphere (35 to 50 km), increase to a peak value in the mid-altitude between 20 to 30 km, and decrease rapidly to a low value in the tropopause below 15 km, and revert back slightly at the bottom stratosphere at 10 km, above the tropical area. The peak ozone abundance of 21 mPa at 22 km or 9.7 ppm at 30 km is referred to as the richest ozone layer in the stratosphere. The parallel competing

diffusion-convection-reaction processes dictating the shape and values of the ozone layer in the stratosphere were elaborated and explained in details.

In the entire stratosphere from 10 km to 50 km above the equator, the calculated ozone distribution displays a similar profile and trend, compared to the measured results. The average ozone abundance of calculations, in either mPa or ppm, was found to be slightly above the measured average by 12% (ppm) or 23% (mPa). The standard deviation of the differences between calculated and measured data was close to 0.25. The simple approach and calculations in this paper are shown to be useful for providing an initial insight into the structure and behavior of the complex ozone layer.

As shown in **Figures 5(a)-(c)**, a sensitivity study of gas diffusivities of molecular ozone D_3 and atomic oxygen D_1 on changing the ozone abundance and profile in the stratosphere showed that in the lower one-third of the stratosphere, both D_1 and D_3 were found to exhibit a negligible impact on ozone values and profile. However, in the upper two-thirds of the stratosphere, D_1 evidently exhibited a pronounced impact on ozone values than D_3. In the upper one-third of the stratosphere, the impact of D_1 on ozone can exceed 24-fold, larger than that of D_3. The mechanism leading to this finding was also elaborated.

Acknowledgements

The authors would like to thank the insightful discussions and inputs from Drs. A. Wolfe, T. Tongele, and B. Marchetti of Catholic University of America's Climate Change Initiatives of Engineering Center for Care of Earth, and the supports from Department of Mechanical Engineering.

Conflicts of Interest

The authors declare no conflicts of interest regarding the publication of this paper.

References

[1] Salawitch, R.J., Fahey, D.W., Hegglin, M.I., McBride, L.A., Tribett, W.R. and Doherty, S.J. (2019) Twenty Questions and Answers about the Ozone Layer: 2018 Update—Scientific Assessment of Ozone Depletion: 2018. World Meteorological Organization, Geneva.

[2] Wei, L., Alelmi, I. and Nieh, S. (2019) Ozone Hole, Where and Size, Bad and Good. Poster Presentation at CUA Research Day, Washington DC.

[3] Wei, L., Alelmi, I. and Nieh, S. (2020) Atmospheric Chemistry and Magnetic Field. Oral Presentation at CUA Research Day, Washington DC.

[4] Molina, M.J. and Rowland, F.S. (1974) Stratospheric Sink for Chlorofluoromethanes: Chlorine Atom-Catalysed Destruction of Ozone. *Nature*, **249**, 810-812. https://doi.org/10.1038/249810a0

[5] Newman, P.A. and Lait, L.R. (2023) NASA Ozone Watch—Images, Data, and Information for Atmospheric Ozone. NASA-Goddard Space Flight Center, Greenbelt. https://ozonewatch.gsfc.nasa.gov/Scripts/big_image.php?date=2023-05-18&hem=S&section=HOME

[6] Solomon, S.C. (1999) Stratospheric Ozone Depletion: A Review of Concepts and History. *Reviews of Geophysics*, **37**, 275-316. https://doi.org/10.1029/1999RG900008

[7] Froidevaux, L. anderson, J., Wang, H.J., Fuller, R., Schwartz, M., Santee, M., Livesey, N., Pumphrey, H., Bernath, P., Russell, J. and McCormick, M. (2015) Global OZone Chemistry and Related Trace Gas Data Records for the Stratosphere (GOZCARDS): Methodology and Sample Results with a Focus on HCl, H_2O, and O_3. *Atmospheric Chemistry and Physics*, **15**, 10471-10507. https://doi.org/10.5194/acp-15-10471-2015

[8] Holton, J.R. and Wehrbein, W.M. (1980) A Numerical Model of the Zonal Mean Circulation of the Middle Atmosphere. *Pure Applies Geophysics*, **118**, 284-306. https://doi.org/10.1007/BF01586455

[9] McCormick, M.P., Veiga, R.E. and Chu, W.P. (1999) Stratospheric Ozone Profile and Total Ozone Trends Derived from the SAGE I and SAGE II Data. *Geophysics Research Letter*, **19**, 269-272. https://doi.org/10.1029/92GL00187

[10] Randel, W.J., Garcia, R.R., Calvo, N. and Marsh, D. (2009) ENSO Influence on Zonal Mean Temperature and Ozone in the Tropical Lower Stratosphere. *Geophysics Research Letter*, **36**, L15822. https://doi.org/10.1029/2009GL039343

[11] Rawcliffe, R.D. and Elliott, D.D. (1966) Latitude Distribution of Ozone at High Altitudes, Deduced from a Satellite Measurement of the Earth's Radiance at 2840 A. *Journal of Geophysical Research*, **71**, 5077-5089. https://doi.org/10.1029/JZ071i021p05077

[12] Prather, M. and Jaffe, A.H. (1990) Global Impact of the Antarctic Ozone Hole: Chemical Propagation. *Journal of Geophysical Research*, **95**, 3473-3492. https://doi.org/10.1029/JD095iD04p03473

[13] Makungu, J., Haario, H. and Mahera, W.C. (2012) A Generalized 1-Dimensional Particle Transport Method for Convection Diffusion Reaction Model. *Afrika Matematika*, **23**, 21-39. https://doi.org/10.1007/s13370-011-0007-0

[14] Siegel, R. and Howell, J.R. (2002) Thermal Radiation Heat Transfer. 4th Edition, Taylor & Francis, New York.

[15] Holton, J.R., Haynes, P.H., Mcintyre, M.E., Douglass, A.R., Rood, R.B. and Pfister, L. (1995) Stratosphere-Troposphere Exchange. *Reviews of Geophysics*, **33**, 403-439. https://doi.org/10.1029/95RG02097